Case Studies in Construction Materials 23 (2025) e05275

Contents lists available at ScienceDirect

Case Studies in Construction Materials

journal homepage: www.elsevier.com/locate/cscm

Rheological properties and aging resistance of asphalt modified with Camellia oleifera fruit shells

Dikuan Wang [a], Chengdong Xia [a,b,c,*], Ge Xiao [d], Duyang Liu [a], Shuangshuang Wang [e], Songtao Lv [a,c], Jinguo Liu [a], Bowen Liu [a], Xin Jin [a]

[a] National Engineering Laboratory of Highway Maintenance Technology, Changsha University of Science & Technology, Changsha, China
[b] Department of Civil and Environmental Engineering, The Hong Kong Polytechnical University, Hung Hom, Hong Kong
[c] Xiangjiang Laboratory, Changsha 410205, China
[d] Modern Investment Co., Ltd., Changsha, China
[e] College of Architecture and Engineering,Yunnan Agricultural University, Kunming 665099, China

ARTICLE INFO

Keywords:
Pavement engineering
Biomass-modified asphalt
Rheological performance
Discarded Camellia oleifera fruit shell

ABSTRACT

The increasing traffic demand and sustainability concerns associated with polymer-modified asphalt present new challenges for road engineering. This study explores the use of discarded Camellia oleifera fruit shells (CFS) as a biomass modifier to produce asphalt with varying CFS contents. The rheological and aging properties of the modified asphalt were evaluated using Dynamic Shear Rheometer (DSR), Bending Beam Rheometer (BBR), and Fourier Transform Infrared Spectroscopy (FTIR). The results show that CFS significantly enhances high-temperature rutting resistance by increasing the complex modulus and deformation stability. A moderate CFS content improves low-temperature ductility and crack resistance, while aging resistance is also notably enhanced. Mechanistic analysis suggests that these improvements are due to the modulus-enhancing effect of lignin, the lubricating properties of polyphenols, and their combined antioxidant effects. The optimal CFS dosage is approximately 12 % by weight. Overall, this study demonstrates that incorporating CFS not only improves asphalt performance but also provides a sustainable approach for biomass waste valorization and the development of environmentally friendly road materials.

1. Introduction

By the end of 2024, China's total highway mileage had reached 5.4904 million kilometers, including 190,700 kilometers of expressways, the majority of which utilize asphalt pavement structures. The country has established the world's largest and most comprehensive expressway network. With this rapid expansion, road construction in China is increasingly oriented toward greener, more resilient, intelligent, durable, and energy-integrated infrastructure [1]. In alignment with national goals for "carbon peaking" and "carbon neutrality," green highways have become a major focus of research and policy development. The European Union enacted the European Climate Law in 2020, targeting carbon neutrality by 2050, while China has committed to peaking carbon emissions by 2030 and achieving carbon neutrality by 2060 as part of its "dual carbon" strategy [2].

* Corresponding author at: National Engineering Laboratory of Highway Maintenance Technology, Changsha University of Science & Technology, Changsha, China.
E-mail address: xiachengdong@stu.csust.edu.cn (C. Xia).

https://doi.org/10.1016/j.cscm.2025.e05275
Received 1 July 2025; Received in revised form 4 September 2025; Accepted 5 September 2025
Available online 9 September 2025

Currently, styrene–butadiene–styrene (SBS)-modified asphalt is widely employed to improve pavement performance under both high- and low-temperature conditions. However, despite its proven effectiveness, SBS is a petroleum-derived material whose production is energy-intensive and resource-dependent, raising significant sustainability concerns [3–5]. In light of global and national initiatives emphasizing carbon neutrality and resource efficiency, these limitations highlight the urgency of developing environmentally friendly alternatives. To address this challenge, biomass-derived modifiers—such as lignin, bio-oils, and biochar—have been proposed as promising substitutes. Each exhibits distinct trade-offs: bio-oils typically enhance low-temperature flexibility; biochar improves high-temperature stiffness but may reduce low-temperature performance; and lignin provides antioxidant benefits while increasing stiffness [6,7]. In practice, biomass-modified asphalt often incorporates bio-oils, biofibers, or bio-ash [3,8–11], replacing part of the petroleum-based components. Previous studies have shown that such modifications can significantly enhance aging resistance, fatigue durability, and overall service life of asphalt pavements [12–16]. Consequently, the partial substitution of petroleum-based materials with biomass alternatives has emerged as a viable pathway toward sustainable and circular development.

Camellia oleifera, a major woody oil crop in southern China, produces large amounts of fruit shells (CFS) as a by-product of oil extraction, and improper disposal of this biomass not only wastes resources but also contributes to environmental pollution [17,18]. Owing to its rich composition of cellulose, hemicellulose, lignin, and phenolic compounds such as tannins and flavonoids [19–21], CFS demonstrates strong potential in asphalt modification. Among these components, lignin is known to enhance the high-temperature rheological properties of asphalt and delay oxidative ageing, though excessive contents may impair fatigue resistance, with recommended dosages generally below 8 % [22,23]. Meanwhile, phenolic compounds characterized by free radical scavenging capacity exhibit strong antioxidative effects, as evidenced by studies on phenol-rich bio-oils, hindered phenol–furfural systems, olive leaf extracts, and phenol-based rejuvenators, all of which have been shown to suppress oxidation and ageing while improving the rheological or mechanical performance of asphalt [24–27]. Importantly, unlike pure lignin, CFS integrates cellulose, hemicellulose, and phenolic substances in addition to lignin [28], and this composite nature provides synergistic effects that suggest broader modification potential than lignin alone, thereby forming the foundation for the present study. With its abundant availability, low cost, and renewability, CFS also offers a sustainable alternative to petroleum-based modifiers such as SBS, which are constrained by high energy consumption and resource dependence, and its incorporation into asphalt not only enhances service performance and environmental adaptability but also promotes the high-value utilization of agricultural by-products, aligning with the national “dual-carbon” strategy and underscoring both theoretical and engineering significance.

To elucidate the modification mechanism, this study identifies the chemical components in CFS using Fourier Transform Infrared Spectroscopy (FTIR) spectroscopy and determines the preparation temperature of the modified asphalt based on the pyrolysis characteristics of its organic constituents. A macro–micro evaluation system is established to investigate the rheological properties of CFS-modified asphalt at both high and low temperatures, with CFS dosages of 4 %, 8 %, 12 %, and 16 %. The study further examines the micrometer-scale dispersion of CFS components as a function of dosage, the apparent morphology of the modified asphalt, and changes in its infrared spectra before and after thermo-oxidative ageing, to validate the modification effects. Additionally, the optimal dosage of CFS is identified, and the underlying mechanism influencing the rheological behavior at different temperatures is analyzed and discussed.

2. Materials and methods

2.1. Raw materials

The materials used in this study were collected from local farmers in Huichang County, Jiangxi Province, China. The discarded CFS belonged to the “*Changlin*” variety and were harvested during the Cold Dew solar term, one of China’s 24 traditional solar periods. The collected CFS were thoroughly washed to remove surface dust, then oven-dried at 105 °C for 4 h. After drying, the shells were ground using a high-speed pulveriser and passed through a 200-mesh sieve to enhance their dispersibility in the pure asphalt, its density is approximately 1.27 g/cm^3. The pure asphalt used was Shuanglong 70# paving-grade asphalt, and its properties are listed in Table 1.

The FTIR spectra were collected in ATR mode over a wavenumber range of 4000–400 cm^{-1} , with a resolution of 4 cm^{-1} and 32 scans per sample, followed by baseline correction. This analysis was conducted to identify the main functional groups present in both pure asphalt and CFS, and the corresponding results are presented in Fig. 1.

Table 1
Technical specifications of pure asphalt.

Property		Unit	Specification Value	Measured Value
Penetration (25 °C, 100 g, 5 s)		0.1 mm	60–80	68
Softening point (Ring-and-Ball method)		℃	≥ 46	45
Ductility (15 °C)		cm	≥ 100	101
Density (15 °C)		g/cm^3	—	1.002
Flash point		℃	≥ 200	310
Solubility (trichloroethylene)		%	≥ 99.5	99.8
Dynamic viscosity at 60 °C		Pa·s	≥ 180	200
RTFOT	Mass change	%	±0.8	0.05
	Retained penetration (25 °C)	%	≥ 61	65
	Retained ductility (10 °C)	cm	≥ 6	12

As shown in Fig. 1, in contrast to the infrared spectral features of the pure asphalt, the CFS exhibits several additional absorption peaks at regions a–b, c and d. According to relevant literature, the broad absorption peaks at a–b are attributed to O-H stretching vibrations, which are broadened due to hydrogen bonding interactions. In the carbonyl region (≈1685–1750 cm^{-1}), two partially overlapping sub-bands can be distinguished. The lower wavenumber component (≈1685–1715 cm^{-1}) arises from the stretching vibrations of conjugated or aromatic carbonyl (C═O) groups, attributable to lignin-derived conjugated and aromatic carbonyl structures. The higher wavenumber component (≈1730–1750 cm^{-1}) corresponds to non-conjugated ester C═O groups, consistent with ester functionalities of polyphenols and tannins, with a possible contribution from minor aliphatic esters.

These findings confirm that the CFS modifier derived from the "*Changlin*" cultivar used in this study contains similar functional components—such as lignin, polyphenols, and tannins—as those identified by Xiang [21] in other cultivars, including "*Huashuo*," "*Huajin*," and "*Xianglin 210*."

2.2. Experimental instruments

For details on the equipment used in the experiments of this study, including model numbers, please refer to Table 2.

2.3. Preparation and characterisation methods for modified asphalt

2.3.1. Preparation of modified asphalt

The main components of CFS are lignin, polyphenols, and oils, with their respective pyrolysis temperature ranges being: 150–900 °C for lignin [29], 200–800 °C for polyphenols [30,31], and gradual thermal decomposition of CFS oils beginning at 134 °C, with significant weight loss occurring above 160 °C and peaking between 200–250 °C [32]. Therefore, for this type of biomass material, it is crucial to select and strictly control the preparation temperature during the asphalt modification process. Based on thermal behaviour, the optimal preparation temperature was set at 150 °C. The preparation procedure for the CFS-modified asphalt is illustrated in Fig. 2**.b**.

To investigate the high- and low-temperature rheological properties of CFS-modified asphalt and to elucidate its modification mechanism, modified asphalt samples were prepared with varying CFS contents. The specific proportions of the modifier used in each formulation are shown in Table 3.

2.3.2. Testing programme for modified asphalt

To provide a clear framework, this study will analyze the characteristics and modification mechanism of CFS, design a testing programme to evaluate its performance, and interpret the results to verify its potential as a sustainable asphalt modifier.

1. Conventional Performance Tests

The penetration test was conducted at 25 °C using a 100 ± 0.05 g standard needle applied for 5 s, in accordance with the Specifications and Test Methods of Bitumen and Bituminous Mixtures for Highway Engineering (JTG E20–2011), to assess the hardness, consistency, and temperature sensitivity of asphalt. The softening point test involved conditioning samples at 5 ± 0.5 °C for 15 min, followed by heating at a rate of 5 ± 0.5 °C/min until the steel ball dropped onto the baseplate. Low-temperature performance was evaluated using the ductility test at 10 °C with a pulling rate of 5 ± 0.25 cm/min. Each test was conducted in triplicate to ensure result reliability.

2. Rheological Characterisation of Modified Asphalt

As a viscoelastic material, asphalt exhibits behaviour highly dependent on temperature and shear rate. A DSR was used to conduct temperature sweep tests from 52 °C to 76 °C. High-temperature performance was assessed by the complex shear modulus (G^*) and rutting factor ($G^*/\sin\delta$). The MSCR test at 58 °C was used to evaluate elasticity improvement, with key parameters including the creep

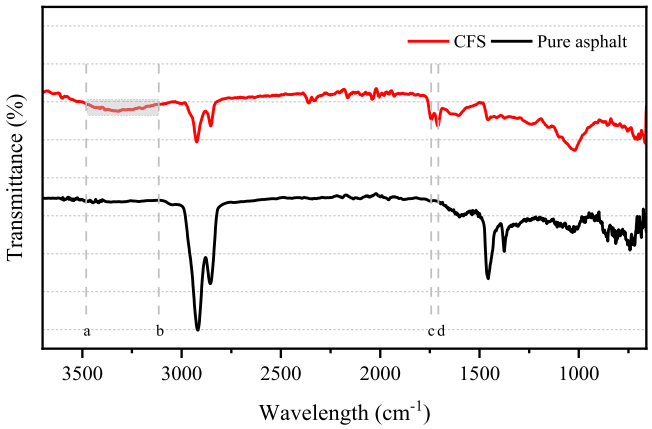

Fig. 1. FTIR Spectra Comparison of CFS and 70# Pure Asphalt.

Table 2
Equipment Used in the Experiments.

Equipment Name	Model
Forced-air drying oven	BPG−9106A
High-speed grinder	DFT−200
High-shear emulsifier	JRJ300-SL
High-speed disperser	GFJ−0.4 A
Softening point tester	SYD-2806F
Penetration tester	SYD-2801F
Ductility tester	SYD-4508C
Rolling Thin Film Oven (RTFOT)	Model 85
Dynamic Shear Rheometer (DSR)	SmartPave 102e
Bending Beam Rheometer (BBR)	TE-BBR SD
Fourier transform infrared spectrometer (FTIR)	Nicolet iS20
Fluorescence microscope (FM) (motorised)	CX3-MDR
Scanning electron microscope (SEM)	Sigma 360

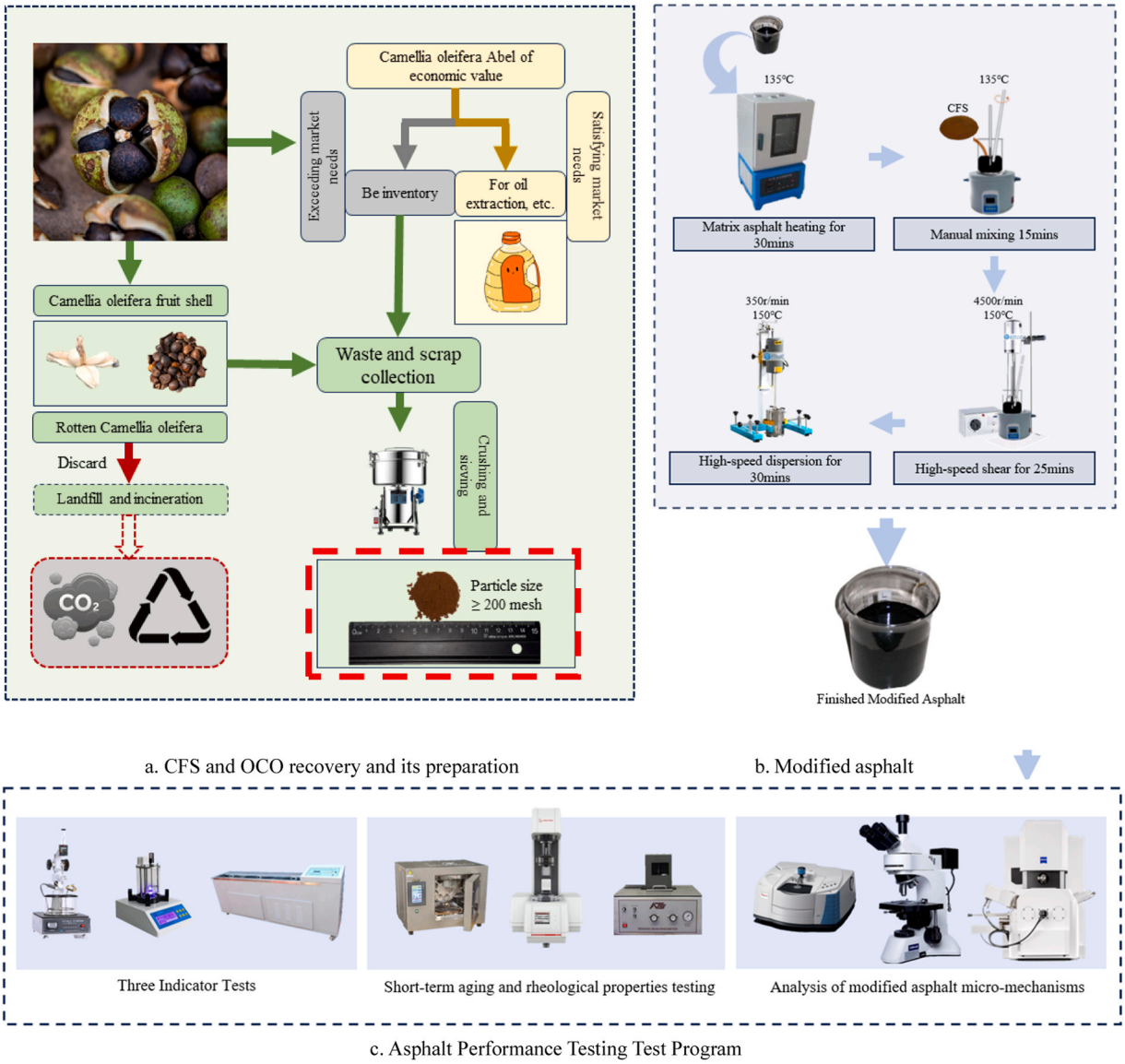

Fig. 2. Main flowchart of the article.

Table 3
CFS/Pure Asphalt Mass Ratio.

Modifier	Mass Ratio to Pure Asphalt			
CFS	4 %	8 %	12 %	16 %

recovery rate (R) and the non-recoverable creep compliance (J_{nr}), the latter being closely associated with rutting resistance [33]. Low-temperature crack resistance was assessed by the BBR test at −6 °C and −12 °C, using stiffness modulus (S) and creep rate (m) as evaluation indices.

3. Microscopic Analysis of Modified Asphalt

FM was employed to observe the morphology and distribution of CFS within the pure asphalt under UV excitation at a wavelength of 365 nm, enabling visual characterisation of modifier dispersion. SEM analysis was performed at an accelerating voltage of 15 kV, providing detailed microstructural images of raw CFS and CFS-modified asphalt by analysing signals from electron–sample interactions, which helped to infer potential performance effects. FTIR spectroscopy was used to identify functional groups based on their characteristic absorption of infrared radiation within the range of 4000–400 cm^{-1} , with a resolution of 4 cm^{-1} and averaging 32 scans. Compared to conventional dispersive IR spectroscopy, FTIR offers higher resolution, sensitivity, and efficiency with reduced interference.

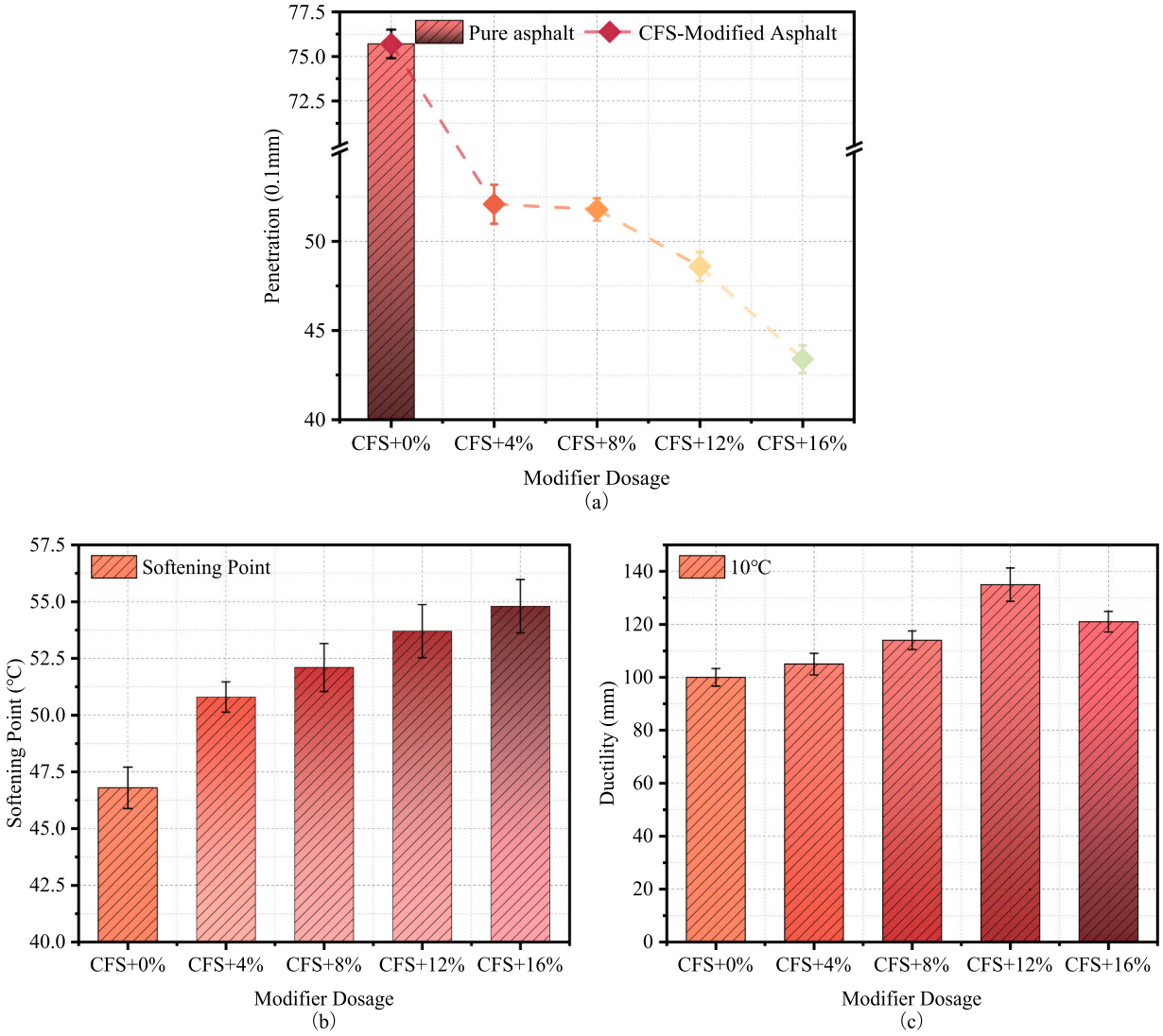

Fig. 3. Influence of CFS Dosage on Penetration, Softening Point, and Ductility.

3. Results and discussion

3.1. Physical properties

To evaluate the basic performance of CFS-modified asphalt, penetration, softening point, and ductility were tested at different dosages. The results are shown in Fig. 3.

As depicted in Fig. 3**(a)**, the penetration values of CFS-modified asphalt are consistently lower than those of the pure asphalt across all dosages. Furthermore, penetration values decrease progressively with increased CFS content. This indicates that adding CFS produces a stiffer, more viscous asphalt binder, thereby enhancing resistance to high-temperature deformation. Similarly, Fig. 3**(b)** illustrates a noticeable increase in the softening point upon CFS incorporation, indicating enhanced high-temperature stability of the modified asphalt. This trend aligns with the penetration test findings. To further evaluate the influence of CFS on low-temperature performance, ductility tests were conducted at 10 °C. Fig. 3**(c)** demonstrates that CFS incorporation improves asphalt ductility. Compared to the pure asphalt, CFS-modified asphalt exhibits higher ductility at all dosages. However, with increasing CFS content, ductility initially rises and subsequently declines. This trend indicates that ductility at low temperatures reaches its peak at a 12 % dosage, followed by a slight reduction at higher contents, potentially related to the internal particle distribution within the binder—a point further examined in the subsequent microstructural analysis.

3.2. Rheological performance evaluation of modified asphalt

3.2.1. Temperature sweep

Fig. 4 illustrates the temperature-dependent variations in the rutting factor ($G^*/\sin\delta$) and phase angle (δ) for CFS-modified asphalt at 10 rad/s. A higher rutting factor indicates improved resistance to deformation. At 58 °C, the pure asphalt exhibited a rutting factor of 6001.24 Pa, which significantly increased upon the addition of CFS, with further increases observed at higher CFS contents. With increasing temperature, the rutting factor decreased across all samples, and the rate of decrease surpassed the incremental increases provided by additional CFS content. This finding indicates that although CFS enhances high-temperature stability, the improvement remains temperature-sensitive. The phase angle δ also increased with temperature, albeit less significantly compared to the rutting factor.

Fig. 5 demonstrates that after RTFOT ageing, the impact of CFS content on the rutting factor becomes more pronounced compared to the unaged samples presented in Fig. 4. At 52 °C, the rutting factor of the pure asphalt increased by 97.53 %, attributed to the loss of lighter fractions and the formation of resins and asphaltenes during ageing. CFS-modified asphalt samples exhibited lower increases—84.14 %, 46.06 %, 47.18 %, and 72.14 %—indicating enhanced anti-ageing performance. This improvement is attributed to lignin and tannins present in CFS. The hydroxyl and methoxy groups of lignin neutralise free radicals [22,34–36], while the polyphenolic hydroxyl structures of tannins provide strong antioxidant activity [37]. Gao et al. [23] demonstrated that lignin improves the high-temperature rheological and fatigue properties of asphalt, thereby supporting its role in resisting thermal-oxidative ageing.

Notably, the ageing index does not consistently decrease with increasing CFS dosage. As depicted in Fig. 5, the ageing index initially declines and subsequently rises, reaching its lowest value at 12 % CFS, indicating that in addition to improving high-temperature performance, this dosage achieves the most favorable resistance to thermal-oxidative aging. At higher contents, although high-temperature stability continues to improve marginally, the overall performance gain becomes limited. This rebound—while still yielding values lower than those of the pure asphalt—may be linked to particle agglomeration at higher CFS dosages, which reduces dispersion uniformity and, in turn, constrains the modification effect. This potential mechanism will be verified in the subsequent FM

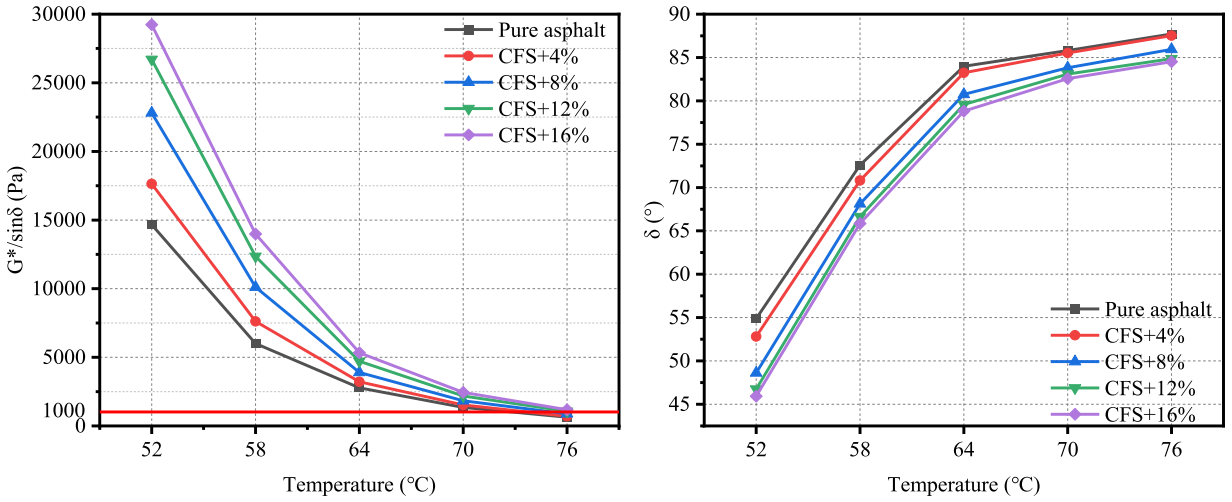

Fig. 4. Effect of CFS Dosage on G/sin δ and Phase Angle.

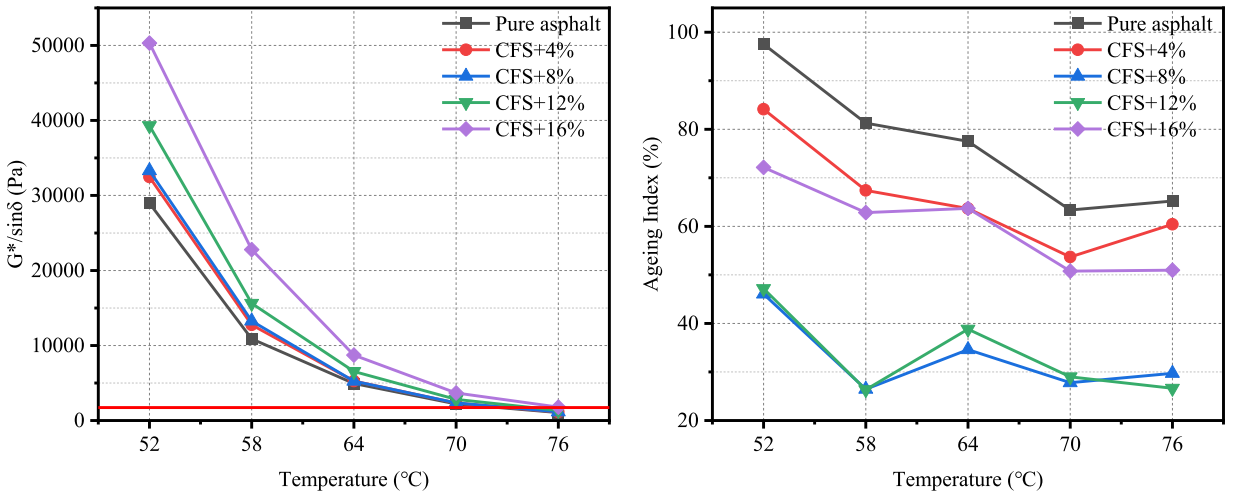

Fig. 5. Effect of CFS Dosage on Rutting Factor and Ageing Index after RTFO Ageing.

analysis.

Fig. 6 illustrates the variation of the complex shear modulus (G^*) with temperature. The modulus (G^*) increases with increasing CFS content, indicating enhanced stiffness. However, the rate of increase slows between 8 % and 12 % CFS content, suggesting a shift in the dominant component. At lower dosages, lignin makes the primary contribution to modulus enhancement. With further increases in dosage, the relative role of polyphenols becomes more apparent, as they improve flowability and help alleviate stress concentrations at the modifier–asphalt interface [27,38], thereby moderating the rate of increase in G^*.

3.2.2. *Frequency sweep*

As illustrated in Fig. 7, the complex shear modulus (G^*) of CFS-modified asphalt was measured at 58 °C across eight loading frequencies. The incorporation of CFS generally increased G^* relative to the pure asphalt, showing an approximately linear trend on a logarithmic frequency scale, attributed to the stiffening effect of lignin. For example, at 8 wt% CFS, G^* increased by 16.02–132.64 % over the frequency range from 0.10 Hz to 15.9 Hz. However, at 0.0159 Hz, the 4 wt% and 8 wt% CFS-modified samples exhibited slightly lower G^* values than the pure asphalt, indicating a decline in stiffness under prolonged loading. This behavior is attributed to enhanced viscous effects, where polyphenols in CFS may improve flowability and thus reduce stiffness. As the frequency increases, elastic response becomes dominant, and the stiffening effect of CFS is more pronounced.

Fig. 8 and Fig. 9 present the master curves of complex shear modulus (G^*) and phase angle (δ) for CFS-modified asphalts at varying dosages, which were constructed using the Williams–Landel–Ferry (WLF) equation with a reference temperature of 58 ℃. Regardless of CFS content, G^* increases with frequency, indicating that the modified asphalt exhibits enhanced elasticity and deformation resistance at low temperatures. This observation aligns with earlier findings showing that modified asphalts display higher G^* values

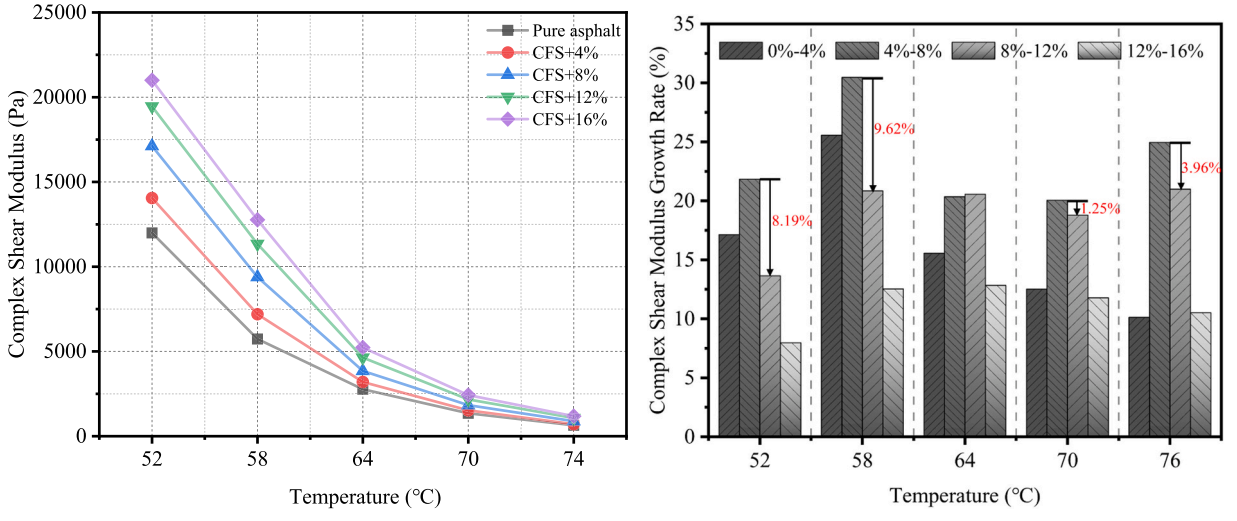

Fig. 6. Change in complex shear modulus (G*) of CFS-modified asphalt with increasing CFS content.

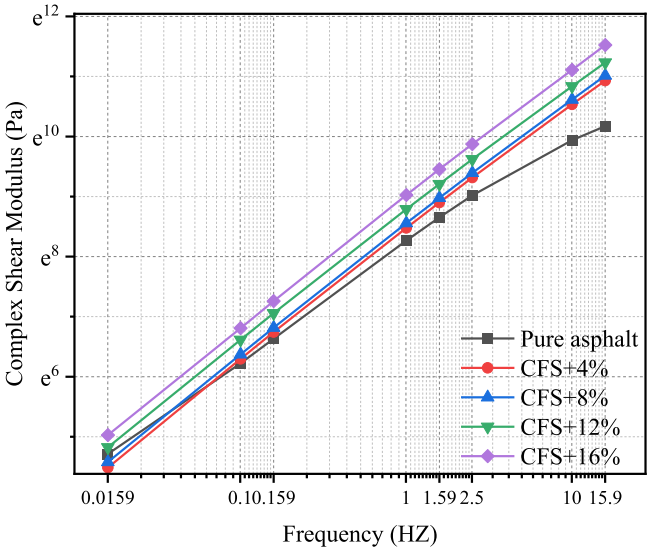

Fig. 7. Complex shear modulus (G*) versus frequency at 58 ℃ for CFS-modified asphalt with varying contents.

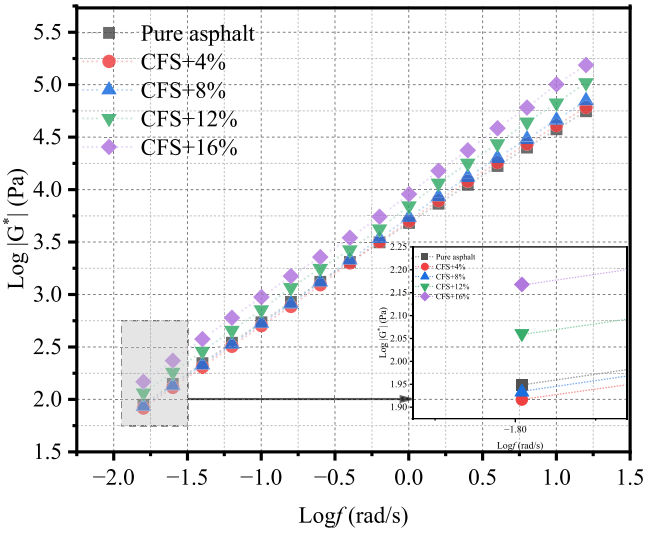

Fig. 8. Master curve of complex shear modulus (G*) at 58 ℃ for CFS-modified asphalt at different CFS dosages.

and rutting factors under cooler conditions.

In Fig. 8, it can be seen that while differences in G^* among the samples are minimal at low frequencies, they become increasingly pronounced as frequency rises. Notably, at low frequencies, the G^* values of the 4 wt% and 8 wt% CFS-modified asphalts are even lower than those of the pure asphalt, consistent with the trend observed in Fig. 7. This behavior is attributed to the presence of polyphenols in CFS, which enhance the binder's viscous response under prolonged loading. As frequency increases, elastic behavior becomes dominant, and the G^* of the modified binders increases accordingly, even if initially lower than that of the pure asphalt.

Fig. 9 further substantiates the previously observed effects of polyphenols and lignin. As the CFS content increases, the phase angle (δ) generally decreases, indicating a trend toward enhanced elasticity. However, at low frequencies, the 4 wt% CFS sample still exhibits a slightly higher δ value than the pure asphalt. In the frequency range of −2.2–0.5 rad/s, the rate of δ reduction becomes more pronounced, suggesting a progressive transition toward elastic behavior. When synthesizing the trends across the entire frequency spectrum, it is evident that the 12 % dosage maintains relatively high stiffness under high-frequency loading while avoiding marked embrittlement under low-frequency conditions. This balance reflects superior compatibility between high- and low-temperature performance compared with other dosages.

3.2.3. Evaluation of high-temperature rheological properties using MSCR

To evaluate the deformation characteristics and elastic recovery of CFS-modified asphalt under repeated traffic loads, Multiple

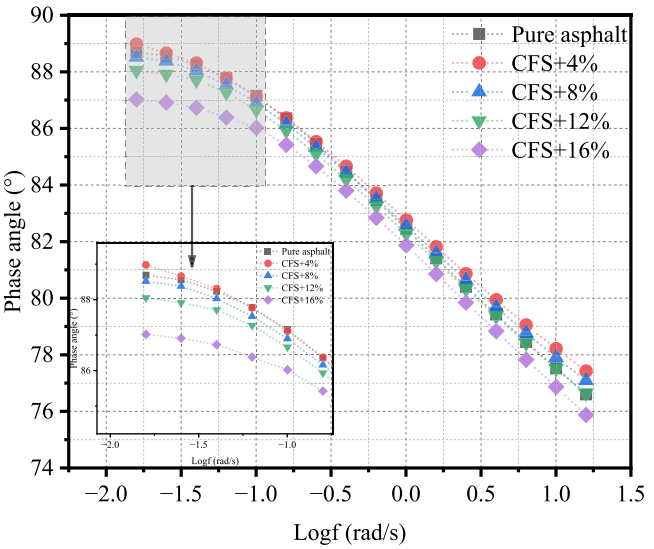

Fig. 9. Master curve of phase angle (δ) at 58 ℃ for CFS-modified asphalt at different CFS dosages.

Stress Creep Recovery (MSCR) tests were performed at two stress levels (0.1 kPa and 3.2 kPa). The results are presented in Figs. 10 and 11.

As illustrated in Fig. 10, all asphalt samples exhibited low shear strain under a 0.1 kPa stress during the initial 200 s, followed by a sharp increase under a 3.2 kPa stress during the final 100 s, reflecting typical pavement behavior under escalating traffic loads. The incorporation of CFS significantly reduced shear strain across this stress range, indicating enhanced resistance to deformation. At 100 s under 3.2 kPa stress, the CFS-modified asphalts demonstrated shear strain reductions of 36.84 %, 46.13 %, 82.85 %, and 90.48 % relative to the pure asphalt, underscoring the considerable improvement in rutting resistance. Furthermore, the CFS-modified asphalts exhibited higher recovery rates and lower non-recoverable creep compliance, providing additional evidence that CFS enhances the elastic response of the binder.

Fig. 11 presents the non-recoverable creep compliance (J_{nr}) and recovery rate (R) of CFS-modified asphalt at 58 °C. At both 0.1 kPa and 3.2 kPa stress levels, J_{nr} decreased significantly with increasing CFS content, indicating enhanced resistance to permanent deformation. The recovery rate (R) also increased with CFS dosage under both stress conditions. At 0.1 kPa, the rate of increase in R slowed at higher dosages, consistent with earlier observations. At 3.2 kPa, this trend was less pronounced, although R generally continued to rise. In particular, the 12 % dosage achieves a favorable balance between recovery rate and non-recoverable creep compliance, whereas further increases in dosage yield only limited additional gains, consistent with the observed diminishing marginal benefit at higher contents. This behavior may be attributed to enhanced viscous effects at low stress levels, where polyphenols act as lubricants, initially promoting recovery but diminishing the marginal gain in performance at higher contents.

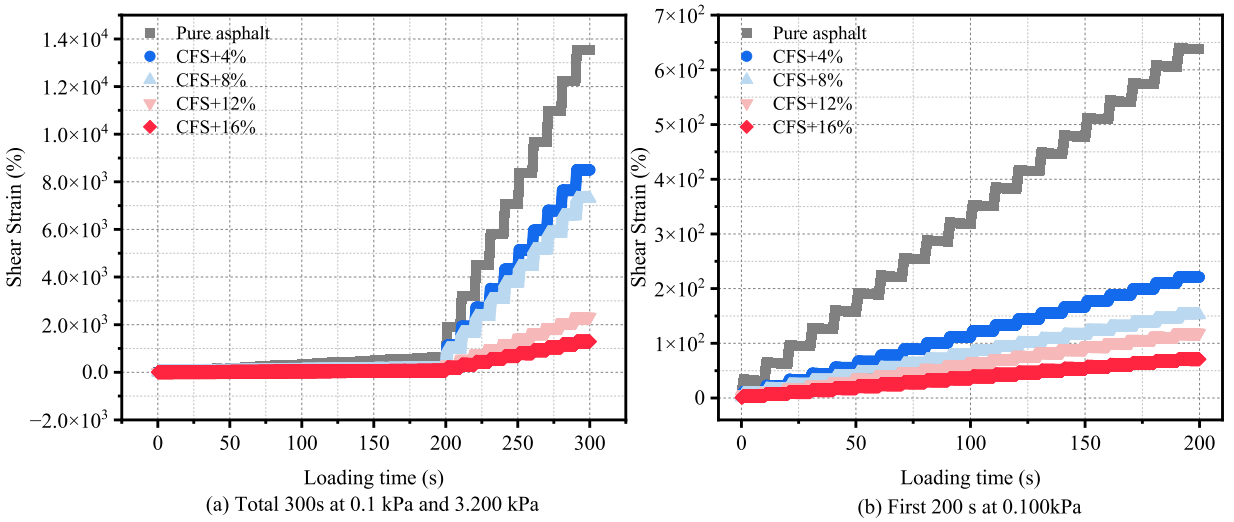

Fig. 10. MSCR test results of CFS-modified asphalt at different stress levels.

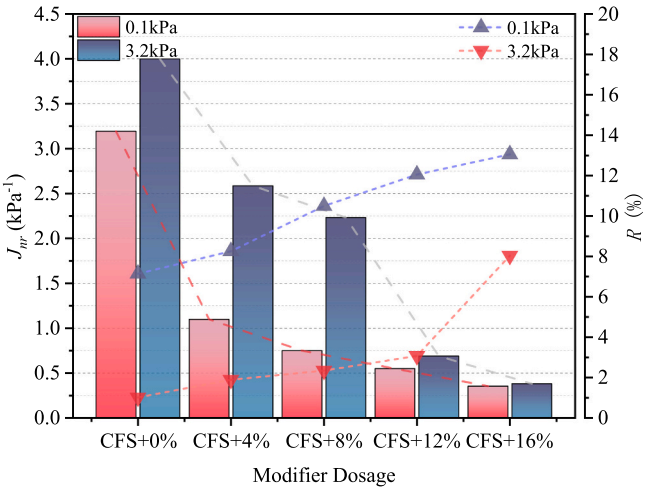

Fig. 11. Non-recoverable creep compliance (J_{nr}) and recovery rate (R) of CFS-modified asphalt.

3.2.4. BBR

The BBR test evaluates the low-temperature cracking resistance of asphalt binders through two parameters: creep stiffness (S) and creep rate (m). A lower S-value indicates higher flexibility and crack resistance, while a higher m-value reflects stronger stress relaxation capacity [39]. Fig. 12 presents the S and m values of CFS-modified asphalt at −6 °C and −12 °C. Unlike lignin-modified asphalt binders, which typically show a monotonic decrease in S and increase in m with dosage [40], the CFS-modified binders displayed a non-monotonous trend. This difference can be reasonably explained by the synergistic effect of lignin and polyphenols in CFS: lignin mainly contributes to stiffening the binder, while polyphenols facilitate stress relaxation, and their concurrent influence leads to the non-monotonic variation observed.

The bending creep results further highlight the dosage- and temperature-dependent effects of CFS on low-temperature asphalt behavior. As shown in Fig. 12, the most evident reduction in stiffness occurred between 4 wt% and 8 wt% at −6 °C, whereas at −12 °C the turning point shifted to between 8 wt% and 12 wt%. This non-monotonic response can be interpreted through the thermodynamic and kinetic characteristics of polyphenolic crystallization. At lower conditioning temperatures, the degree of supercooling is greater, which increases the nucleation driving force ($DT = T_{melt} - T_{cold}$) [41]. A larger DT at −12 °C compared with −6 °C accelerates nucleation and promotes subsequent crystal growth of polyphenolic compounds. The formation of these crystalline domains can locally stiffen the asphalt matrix and restrict molecular mobility, thereby reducing the lubricating effect normally provided by polyphenols. This mechanism explains why the S shows a sharper variation at −12 °C, reflecting the competition between lignin-induced stiffening and polyphenol-driven relaxation. Meanwhile, the 12 wt% dosage consistently provided the most favorable balance between stiffness and relaxation, as indicated by the combined evaluation of S and m values. Notably, the non-coincident turning points of S and m suggest that stiffness and relaxation processes are not equally sensitive to CFS addition, further evidencing the complex interplay between

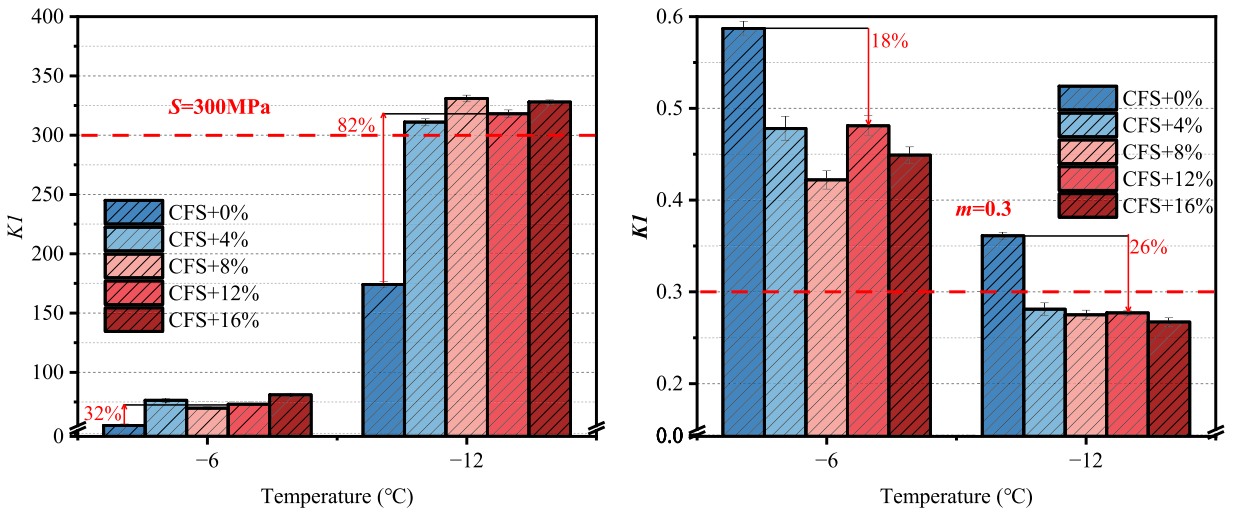

Fig. 12. BBR test results of CFS-modified asphalt at different dosages and low temperatures.

lignin and polyphenols within the asphalt system.

3.3. Microstructural characterisation

3.3.1. FM

This section validates the hypothesis proposed in the earlier performance analysis, where the non-linear trends observed at higher dosages were speculated to be related to particle distribution effects. To visually assess the dispersion state of CFS in asphalt, FM was employed. Fig. 13 (a–d) shows CFS-modified asphalt samples with dosages increasing from 4 % to 16 % (left to right). As CFS content increases, the bright regions characteristic of the pure asphalt decrease noticeably, while dark regions expand and the overall fluorescence intensity progressively declines. At lower dosages, CFS particles are uniformly dispersed, allowing the pure asphalt to retain strong fluorescence. By contrast, at higher dosages, the reduced interparticle spacing promotes localized aggregation, resulting in a marked reduction in fluorescence intensity. This progressive evolution from uniform dispersion at low dosages (4–8 %) to localized aggregation at higher dosages (12–16 %) effectively illustrates the modifier's dispersion and crosslinking state under different dosages. Such microstructural observations directly support the non-linear performance behaviors discussed earlier, confirming that dosage-dependent particle distribution plays a critical role in governing both the high- and low-temperature performance of CFS-modified asphalt.

This attenuation arises from the fluorescence-quenching effect of CFS particles—particularly due to its lignin and polyphenolic constituents—on asphalt's fluorescent moieties. As dosage increases, more quenching centers form, leading to enhanced non-radiative energy transfer and inner-filter effects, consistent with dual static–dynamic quenching mechanisms [42]. In lignin-derived polyphenol systems, increasing non-fluorescent absorber content similarly suppresses autofluorescence [43]. Consequently, higher CFS contents undermine dispersion uniformity and promote aggregation, thereby amplifying quenching and resulting in a progressive decline in fluorescence intensity in the modified asphalt.

3.3.2. SEM

To further examine the microstructural characteristics and surface morphology of both pure and CFS-modified asphalt, SEM was conducted at an accelerating voltage of 8 kV. This technique allows detailed observation of surface texture, particle distribution, and deformation features, thereby offering insights into the physical effects of CFS incorporation at different dosages. Figs. 14 and 15 present SEM images of unmodified asphalt and CFS-modified asphalt, respectively, under varying magnifications and CFS contents.

Fig. 14 shows SEM images of unmodified pure bitumen. Image (a) presents the surface morphology at 50 × magnification, while image (b) shows the same sample at 505 × magnification. Localized bulging, breakage, and extensive cracking are observed after the vacuum and gold-sputtering treatment. During SEM sample preparation, the specimen is vacuumed and coated with gold to enhance conductivity and ensure image clarity. However, under negative pressure during vacuuming, pure bitumen tends to crumple due to its low modulus and poor rheological properties. As a result, it cannot withstand the applied vacuum stress, leading to deformation such as bulging and cracking, which explains the surface features observed in Fig. 14.

Preliminary experiments indicated that the primary constituents of CFS—lignin, polyphenols, and other minor components—exert distinct modification effects on matrix asphalt. Lignin improves the modulus and stiffness of asphalt at elevated temperatures but, due to its rigid nature, may compromise flexibility under low-temperature conditions. In contrast, polyphenols enhance aging resistance and promote molecular mobility, thereby providing a lubricating effect within the asphalt matrix. Fig. 15 presents SEM images of CFS-modified asphalt at dosages of 4 %, 8 %, 12 %, and 16 %. At 4 % (Fig. 15**(a)**), bulging is significantly reduced to approximately 20 μm, accompanied by fewer surface cracks. With higher dosages (Fig. 15**(a)–(d)**), varying degrees of folding are observed, displaying a sparse–dense–sparse distribution pattern, with fold severity in the order of (c) > (d) > (b). This behavior reflects the combined action of lignin and polyphenols: lignin reinforces the matrix and mitigates bulging without fully eliminating it, while polyphenols contribute to lubrication, thereby influencing folding characteristics. Overall, the SEM observations confirm that appropriate CFS incorporation not only modifies surface morphology but also provides microstructural evidence supporting the rheological improvements and non-linear performance trends identified at higher dosages.

3.3.3. FTIR

To verify the incorporation of functional groups from CFS and assess chemical changes in asphalt before and after ageing, FTIR spectroscopy was employed. This technique enables identification of characteristic absorption peaks associated with lignin, polyphenols, and oxidation products. Figs. 16 and 17 display the FTIR spectra of CFS-modified asphalt with varying dosages before and after RTFOT ageing, respectively, providing molecular-level evidence of modification effectiveness and ageing resistance.

As shown in the infrared spectral data in Fig. 16, all new characteristic peaks identified in CFS—compared to pure asphalt—are also present in the CFS-modified asphalt. This finding supports the validity of the preparation method described in Section 2.3.1. The specified preparation temperature effectively preserved the active components of CFS, including lignin, polyphenols, and tannins, while minimizing pyrolytic loss. Furthermore, the retention of CFS-specific characteristic peaks (e.g., carbonyl, and aromatic vibrations) in the CFS-modified asphalt—without the emergence of additional reaction-induced peaks—supports the reliability of our preliminary experimental conclusions regarding performance improvements.

FTIR spectroscopy can be used to assess the ageing degree of asphalt to some extent. By comparing spectra before and after ageing, an ageing index can be calculated to evaluate the extent of oxidative degradation [44]. During natural or simulated ageing, thermal-oxidative reactions increase the number of carbonyl groups in asphalt [45], making the carbonyl index (*CI*) a useful indicator of microstructural changes.

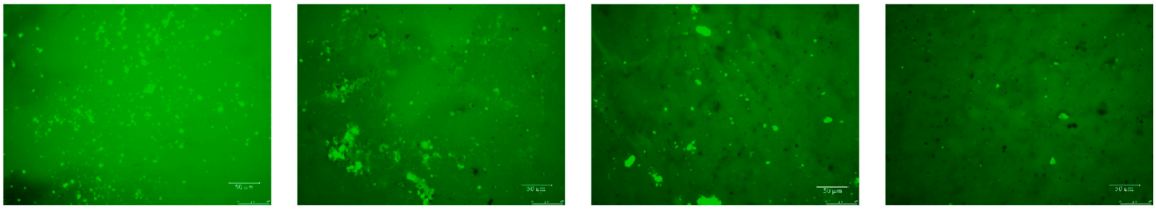

Fig. 13. Fluorescence micrographs of CFS-modified asphalt with varying CFS contents.

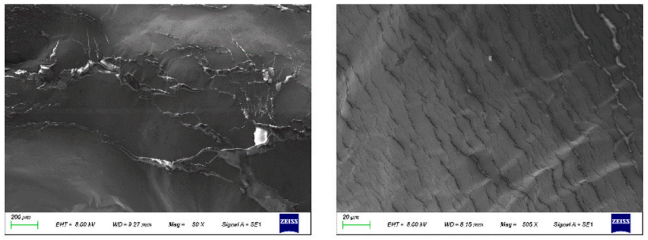

Fig. 14. Scanning electron microscope (SEM) images of pure asphalt at 50 × and 505 × magnification.

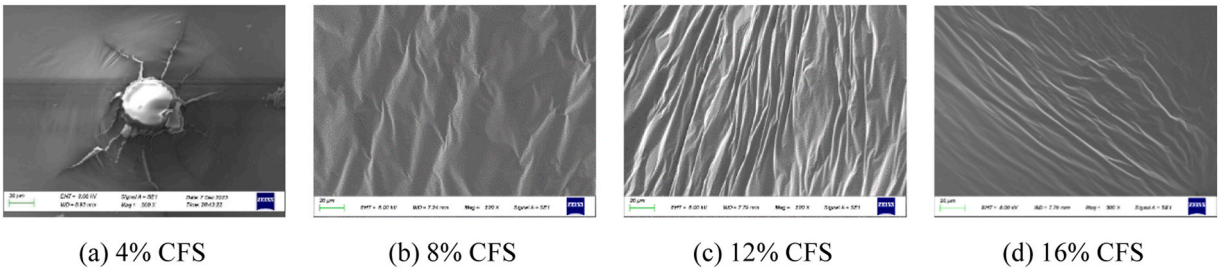

Fig. 15. SEM images of CFS-modified asphalt at different CFS dosages.

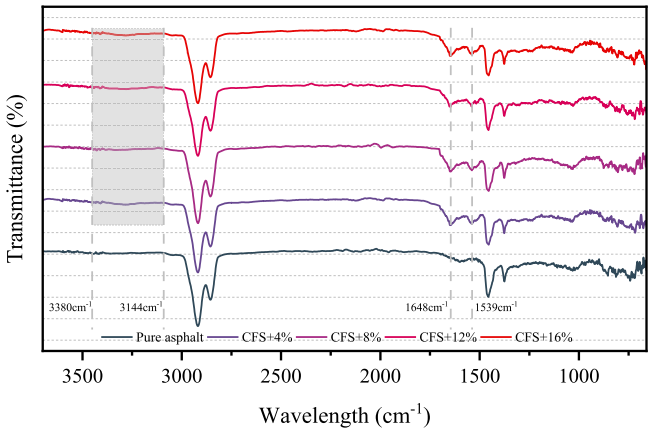

Fig. 16. FTIR spectra of CFS-modified asphalt with varying CFS contents.

$$CI = \frac{\sum \text{AreaofC} = \text{O}(1700\text{cm}^{-1})}{\sum \text{AreaofC} - \text{H}(1456\text{cm}^{-1})} \quad (1)$$

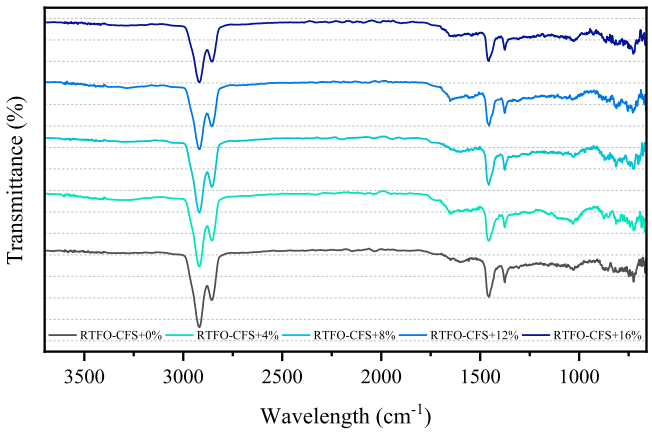

Fig. 17. FTIR spectra of CFS-modified asphalt with varying dosages after RTFO short-term ageing.

The ageing indices (*CI*) of CFS-modified asphalt at different dosages were calculated, as shown in Table 4.

Analysis of the *CI* index for CFS-modified asphalt at various dosages indicates that CFS improves the thermo-oxidative aging resistance of pure asphalt, as evidenced by the reduced conversion of C–H to C═O bonds under thermo-oxidative conditions. This enhancement arises from lignin and tannins in CFS, whose polyphenolic hydroxyl and methoxy groups can scavenge free radicals generated during aging, thereby mitigating oxidative degradation. The *CI* index across groups I to V first decreases and then increases with higher CFS contents. FM observations in Fig. 13 confirm that this rebound at higher dosages results from particle agglomeration and reduced dispersion uniformity, which diminish the antioxidant effectiveness of CFS. Considering both the *CI* index and the rheological performance trends, the 12 % dosage marks the point where gains in high- and low-temperature properties align with the greatest improvement in thermal-oxidative aging resistance, identifying it as the most balanced formulation among the dosages studied.

4. Conclusion

In this study, Camellia oleifera fruit shell (CFS) was utilized as a biomass modifier to prepare CFS-modified asphalt at dosages of 4 %, 8 %, 12 %, and 16 %. The properties and modification mechanism of the CFS-modified asphalt were systematically investigated through temperature sweep, frequency sweep, low-temperature bending creep tests, microscopic observation, and infrared spectroscopy. Based on the results, the main conclusions are summarized as follows:

(1) CFS significantly enhances the high-temperature stability of pure asphalt. Increased dosage improves penetration, softening point, rutting factor ($G^*/\sin\delta$), and reduces non-recoverable creep compliance, mainly due to the three-dimensional fibrous lignin structure that boosts modulus and deformation resistance.

(2) At low temperatures, CFS-modified asphalt shows better ductility, stiffness, and creep rate. However, these improvements are non-linear, with optimal performance observed at 12 % dosage and a decline at 16 %. Polyphenols play a critical role by lubricating asphalt components, as confirmed by frequency sweep tests, which showed higher viscous behaviour at low frequencies.

(3) FM revealed dispersion issues, with particle agglomeration evident even at 4 % dosage, worsening with higher content and leading to fluorescence quenching. This helps explain the decline in low-temperature performance at high dosages.

(4) FTIR analysis confirmed the presence of lignin and polyphenols in the modified asphalt, supporting the effectiveness of the preparation method. Ageing tests showed a significant reduction in the carbonyl index (*CI*), indicating enhanced ageing resistance, although *CI* also followed a non-linear trend, likely due to limited dispersion at higher dosages.

(5) The 12 % CFS dosage provides near-maximum performance in high-temperature stability, low-temperature crack resistance, and aging resistance, while avoiding the dispersion and low-temperature drawbacks of higher contents. It is therefore recommended as the optimal dosage, with future work focusing on long-term performance under varied climates and synergy with polymer modifiers such as SBS.

In conclusion, CFS-modified asphalt demonstrates promising improvements in both high- and low-temperature performance,

Table 4
Carbonyl index (*CI*) of CFS-modified asphalt at varying dosages.

No.	CFS Dosage (%)	Ageing Method	*CI* Index
I	CFS+ 0 %	RTFOT	0.0634
II	CFS+ 4 %	RTFOT	0.0455
III	CFS+ 8 %	RTFOT	0.0427
IV	CFS+ 12 %	RTFOT	0.0447
V	CFS+ 16 %	RTFOT	0.0451

enhanced rheological behavior, and superior resistance to aging, presenting a sustainable and viable alternative for asphalt modification. This study provides a solid theoretical and technical basis for its potential engineering applications and future development. Nonetheless, certain limitations should be recognized: storage stability, particularly at higher dosages, remains a concern; variability in the intrinsic composition of biomass may introduce performance uncertainties; and the current findings are confined to laboratory-scale evaluations without field validation. These limitations highlight the need for further research aimed at improving compatibility and dispersion while confirming long-term performance under practical service conditions.

CRediT authorship contribution statement

Shuangshuang Wang: Writing – review & editing, Supervision. **Songtao Lv:** Writing – review & editing, Supervision. **Duyang Liu:** Resources, Investigation, Formal analysis. **Chengdong Xia:** Writing – review & editing, Resources. **Ge Xiao:** Visualization, Validation, Supervision. **Dikuan Wang:** Writing – review & editing, Writing – original draft, Validation, Resources, Data curation. **Xin Jin:** Resources, Investigation. **Jinguo Liu:** Resources, Investigation. **Bowen Liu:** Resources, Investigation.

Declaration of Competing Interest

The authors declare the following financial interests/personal relationships which may be considered as potential competing interests: Chengdong Xia reports financial support was provided by The Open Fund of National Engineering Research Center of Highway Maintenance Technology (Changsha University of Science & Technology). Chengdong Xia, Dikuan Wang has patent #ZL 2024 1 0927536.1 with royalties paid to Chengdong Xia, Dikuan Wang. If there are other authors, they declare that they have no known competing financial interests or personal relationships that could have appeared to influence the work reported in this paper.

Acknowledgments

This research is partially sponsored by these agents and organizations: National Outstanding Youth Science Fund Project of National Natural Science Foundation of China (52225806), the Open Fund of National Engineering Research Center of Highway Maintenance Technology (Changsha University of Science & Technology) (kfj230203, kfj230205), Shandong Province Transportation Science and Technology Program (2023B83), the Major R&D project of Zhejiang Provincial Department of Transportation (ZJXL-SJT-202316A).

Data availability

Data will be made available on request.

References

[1] Editorial Dept. of CJHT, A Review of Academic Research on Pavement Engineering in China: 2024, China J. Highw. Transp. 37 (03) (2024) 1–81.
[2] B. Liang, H. Zhang, Y. Liang, X. Wang, J. Zheng, A review of research on warm mix asphalt (WMA) technology, J. Traffic Transp. Eng. 23 (02) (2023) 24–46.
[3] L. He, M. Tao, Z. Liu, Z. Cao, J. Zhu, J. Gao, W.Vd bergh, E. Chailleux, Y. Huang, K. Vasconcelos, A. Cannone Falchetto, R. Balieu, J. Grenfell, D.J. Wilson, J. Valentin, K.J. Kowalski, L. Rzek, L. Gaspar, T. Ling, Y. Ma, Biomass valorization toward sustainable asphalt pavements: progress and prospects, Waste Manag. 165 (2023) 159–178.
[4] Z. Hong, K. Yan, D. Ge, M. Wang, G. Li, H. Li, Effect of styrene-butadiene-styrene (SBS) on laboratory properties of low-density polyethylene (LDPE)/ethylene-vinyl acetate (EVA) compound modified asphalt, J. Clean. Prod. 338 (2022) 130677.
[5] H. Yu, J. Ge, G. Qian, C. Zhang, W. Dai, P. Li, Evaluation on the rejuvenation and diffusion characteristics of waste cooking oil on aged SBS asphalt based on molecular dynamics method, J. Clean. Prod. 406 (2023) 136998.
[6] G.G. Al-Khateeb, S.A. Alattieh, W. Zeiada, C. Castorena, State-of-the-Art review on the behavior of Bio-Asphalt binders and mixtures 29 (16) (2024) 3835.
[7] D. Mehta, N. Saboo, Performance of bio-asphalts: state of the art review, Environ. Sci. Pollut. Res. 30 (57) (2023) 119772–119795.
[8] S. Chen, Y. Wang, X. He, Y. Su, Y. Cao, C. Yang, X. Duan, Mechanically activated shell powder modified asphalt and its aging resistance enhancement, Case Stud. Constr. Mater. 21 (2024) e04023.
[9] N. Su, F. Xiao, J. Wang, L. Cong, S. Amirkhanian, Productions and applications of bio-asphalts – a review, Constr. Build. Mater. 183 (2018) 578–591.
[10] F. Liu, J. Fu, W. Guo, J. Yu, Zn Guo, Q. Ma, F. Yang, A review of the current research on modified Bio-Asphalt, Appl. Chem. Ind. 53 (08) (2024) 1943–1948+1954.
[11] D. Zhang, Y. Zheng, G. Yuan, H. Guo, Q. Zhou, G. Qian, B. Liang, Comparative analysis of rheological and microscopic performance of SBS modified asphalt based on field aging and laboratory aging, Fuel 352 (2023) 128933.
[12] E. Gaudenzi, F. Canestrari, X. Lu, F. Cardone, Performance assessment of asphalt mixture produced with a Bio-Based binder, Materials 14 (4) (2021) 918.
[13] D. Hu, X. Gu, G. Wang, Z. Zhou, L. Sun, J. Pei, Performance and mechanism of lignin and quercetin as bio-based anti-aging agents for asphalt binder: a combined experimental and ab initio study, J. Mol. Liq. 359 (2022) 119310.
[14] R. Zhang, Z. You, J. Ji, Q. Shi, Z. Suo, A review of characteristics of Bio-Oils and their utilization as additives of asphalts, Molecules 26 (16) (2021) 5049.
[15] M. Zeng, H. Pan, Y. Zhao, W. Tian, Evaluation of asphalt binder containing castor oil-based bioasphalt using conventional tests, Constr. Build. Mater. 126 (2016) 537–543.
[16] M. Elkashef, J. Podolsky, R.C. Williams, E. Cochran, Preliminary examination of soybean oil derived material as a potential rejuvenator through superpave criteria and asphalt bitumen rheology, Constr. Build. Mater. 149 (2017) 826–836.
[17] M. Xia, Y. Wang, S. Zhang, Y. Zeng, Y. Liu, R. Ruan, Research progress on the comprehensive utilisation of camellia shells, Biomass.. Chem. Eng. 55 (06) (2021) 26–38.
[18] Z. Yang, L. Fu, F. Fan, Thermal characteristics and kinetics of waste camellia oleifera shells by TG–GC/MS, ACS Omega 4 (6) (2019) 10370–10375.
[19] X. Liu, Y. Wu, Y. Gao, Z. Jiang, Z. Zhao, W. Zeng, M. Xie, S. Liu, R. Liu, Y. Chao, S. Nie, A. Zhang, C. Li, Z. Xiao, Valorization of camellia oleifera oil processing byproducts to value-added chemicals and biobased materials: a critical review, Green. Energy Environ. 9 (1) (2024) 28–53.
[20] L. Wang, Q. Xu, L. Dong, Q. Zhang, J. Tan, Study on the chemical composition of camellia shells, J. Trop. Subtrop. Bot. 25 (01) (2017) 81–86.

[21] X. Xiang, Development of camellia oleifera pericarp and changes in its internal components, Central South University of Forestry and Technology, Changsha, 2023.
[22] K.B. Batista, R.P.L. Padilha, T.O. Castro, C.F.S.C. Silva, M.F.A.S. Araújo, L.F.M. Leite, V.M.D. Pasa, V.F.C. Lins, High-temperature, low-temperature and weathering aging performance of lignin modified asphalt binders, Ind. Crops Prod. 111 (2018) 107–116.
[23] J.F. Gao, H.N. Wang, C.C. Liu, D.D. Ge, Z.P. You, M. Yu, High-temperature rheological behavior and fatigue performance of lignin modified asphalt binder, Constr. Build. Mater. 230 (2020).
[24] F. Pahlavan, A. Lamanna, K.B. Park, S.F. Kabir, J.S. Kim, E.H. Fini, Phenol-rich bio-oils as free-radical scavengers to hinder oxidative aging in asphalt binder, Resour. Conserv. Recycl. 187 (2022).
[25] Y.M. Gao, Y.Q. Zhang, E.L. Omairey, S. Al-Malaika, H. Sheena, Influence of anti-ageing compounds on rheological properties of bitumen, J. Clean. Prod. 318 (2021).
[26] V. Loise, A.A. Abe, M. Porto, I. Muzzalupo, L. Madeo, M.F. Colella, C.O. Rossi, P. Caputo, Plant Waste-Based bioadditive as an antioxidant agent and rheological modifier of bitumen, Materials 17 (10) (2024).
[27] S.A. Liu, H.Z. Wang, J. Yang, Utilization of biomass waste to produce phenol-rich bio-oil for enhancing the long-term aging resistance of rejuvenated bitumen, Mater. Struct. 58 (3) (2025).
[28] W. Quan, A. Wang, C. Gao, C.J.Fi.C. Li, Applications of Chinese camellia oleifera and its by-products, A Rev. 10 (2022) 921246.
[29] L. Yao, L. Ge, C. Zhao, R. Wang, M. Zuo, Y. Zhang, Y. Wang, C. Xu, Research progress on the pyrolytic conversion of lignocellulosic biomass, J. Chin. Soc. Power Eng. 44 (05) (2024) 665–680.
[30] F. Yao, Study on the pyrolysis and oxidation characteristics of tea polyphenol derivatives and their reaction mechanisms, University of Science and Technology of China, Hefei, 2018.
[31] Y. Lu, L. Lu, Study on the thermal properties and pyrolysis kinetics of tannic acid, Chem. Ind. For. Prod. 42 (03) (2022) 83–89.
[32] S. Li, E. Jiang, M. Wang, P. Han, X. Jian, G. Gao, Combustion characteristics of Bio-Oil from multistage condensation of volatiles during continuous pyrolysis of camellia shells, J. Chin. Agric. Mech. 39 (06) (2017) 245–249.
[33] C. Xia, Study on the performance enhancement methods and mechanisms of asphalt modified with waste PP plastics composites, Changsha University of Science & Technology, Changsha, 2022.
[34] M. Azadfar, A.H. Gao, M.V. Bule, S. Chen, Structural characterization of lignin: a potential source of antioxidants guaiacol and 4-vinylguaiacol, Int. J. Biol. Macromol. 75 (2015) 58–66.
[35] T. Dizhbite, G. Telysheva, V. Jurkjane, U. Viesturs, characterization of the radical scavenging activity of lignins—natural antioxidants, Bioresour. Technol. 95 (3) (2004) 309–317.
[36] C.G. Boeriu, D. Bravo, R.J.A. Gosselink, J.E.G. van Dam, Characterisation of structure-dependent functional properties of lignin with infrared spectroscopy, Ind. Crops Prod. 20 (2) (2004) 205–218.
[37] C. Peng, C. Cheng, S. Wen, D. Zhu, H. Shan, Experimental study on the High-Temperature performance of tannic Acid–Modified asphalt based on DSR and RV tests, Sci. Technol. Eng. 19 (28) (2019) 341–346.
[38] H. Zhou, D. Zhang, Preparation and performance analysis of crumb Rubber/Polyphenol-Modified asphalt, Fujian Commun. Technol. 01 (2024) 7–12.
[39] Y. Wang, W. Wang, L. Wang, Understanding the relationships between rheology and chemistry of asphalt binders: a review, Constr. Build. Mater. 329 (2022) 127161.
[40] G. Xu, H. Wang, H. Zhu, Rheological properties and anti-aging performance of asphalt binder modified with wood lignin, Constr. Build. Mater. 151 (2017) 801–808.
[41] S.S. Kontos, P.G. Koutsoukos, C.A. Paraskeva, Removal and recovery of phenolic compounds from olive mill wastewater by cooling crystallization, Chem. Eng. J. 251 (2014) 319–328.
[42] A.S. Tanwar, R. Parui, R. Garai, M.A. Chanu, P.K. Iyer, Dual “Static and Dynamic” fluorescence quenching mechanisms based detection of TNT via a cationic conjugated polymer, ACS Meas. Sci. Au 2 (1) (2022) 23–30.
[43] Z. Yu, D. Xu, J. Hu, S. Chang, G. Liu, Q. Huang, J. Han, T. Li, Y. Liu, X.A. Wang, Improving the autofluorescence of lophira alata woody cells via the removal of extractives, Polymers 15 (15) (2023).
[44] D. Zhang, Y. Zheng, G. Yuan, G. Qian, H. Zhang, Z. You, P. Li, Chemical characteristics analyze of SBS-modified bitumen containing composite nanomaterials after aging by FTIR and GPC, Constr. Build. Mater. 324 (2022) 126522.
[45] S. Werkovits, K. Primerano, M. Bacher, T. Rosenau, B. Hofko, H. Grothe, An analytical framework to assess the chemical changes in polymer-modified bitumen upon natural and simulated ageing, Fuel 381 (2025) 133257.